Collision-Induced Dissociation of Adenine

Chad C. Nelson and James A. McCloskey*

Contribution from the Departments of Medicinal Chemistry and Biochemistry, University of Utah, Salt Lake City, Utah 84112. *Received April 25, 1991*

Abstract: The collision-induced dissociation of protonated adenine, and of adenine monomethylated at positions N-1, C-2, N-3, N^6, and N-7 has been studied by tandem mass spectrometry using models extensively labeled with stable isotopes. These data are used to gain understanding of the mechanisms of dissociation of protonated heterocycles in general, and as a basis for the applications of tandem mass spectrometry to structural studies of adenine derivatives and other nucleic acid constituents. Following collisional activation at 30-eV translational energy under multiple-collision conditions, protonated adenine undergoes decomposition along three independent major pathways which are of minor occurrence in electron ionization mass spectra: (1) expulsion of NH_3, found to be derived in approximately equal proportion from endocyclic N-1 and exocyclic N^6; (2) loss of NH_2CN, derived almost exclusively from N-1–C-6–N^6; and (3) formation of NH_4^+ directly from the protonated molecular ion, originating principally from N-1. A fourth major pathway which is also prevalent in electron ionization mass spectra involves sequential expulsion of three molecules of HCN, which occurs in the first step by highly selective loss of N-1 and C-2. Proposed mechanisms of dissociation are based on initial opening of the pyrimidine ring at N-1–C-6 or at N-1–C-2, resulting from protonation of N-1 in the primary ionization process. Activation of ions under single-collision conditions results in deposition of less internal energy, such that virtually no fragmentation occurs beyond the first step of each of the four principal pathways. Under these conditions greater selectivity in favor of loss of N-1 in expulsion of NH_3 occurs, but with less effect on the other three pathways. Mass spectra of protonated methyladenine isomers and their ^{15}N- and ^2H-labeled analogues strongly support the occurrence of reaction paths analogous to those of adenine, and demonstrate the charge-localized pyrimidine ring to be the initial site of dissociation reactions.

Introduction

Structural modifications of nucleic acid bases play a critical role in RNA and DNA structure and function, both in the case of natural modifications and in the case of those resulting from xenobiotic alteration. Mass spectrometry has been employed effectively in the structural characterization of bases and nucleosides,[1,2] particularly in the case of RNA from various sources[3,4] which is known to contain over 80 different nucleosides, 74 of which are modified in the base by posttranscriptional reactions. One of the most difficult aspects of such work has been the interpretation of the mass spectra of substituted purines, due primarily to the complexity of dissociation reactions represented,[5] and the somewhat limited number of studies in which isotopic labeling has been employed to examine the details of reaction paths in model compounds.[6] In contrast with much earlier work involving electron ionization (EI), the advent in recent years of a variety of desorption ionization methods has raised the question as to the similarity of mechanisms of dissociation of protonated (MH^+) or deprotonated [$(M-H)^-$] molecular ions compared with those generated from EI ($M^{\bullet+}$). The method of choice for study of these reactions is collision-induced dissociation[9] (CID) used in conjunction with tandem mass spectrometry, for two reasons. First, the collision process is an effective means of introducing sufficient internal energy into the protonated purine nucleus to promote extensive fragmentation, which is otherwise minimal in the case of spontaneous dissociation. Second, tandem mass spectrometry is a powerful method for structural characterization studies,[10] in part because CID mass spectra of the component of interest can be measured free of significant interference, directly in biological isolates or reaction mixtures, and because of the broad applicability of desorption ionization techniques to highly polar molecules of biological origin.[11] Although there have been a number of studies of the CID mass spectra of purine nucleosides,[2] these data are of little use for study of the dissociation of the base because nearly all of the collision energy is channeled into cleavage of the glycosidic bond, resulting in little fragmentation of the base. This problem is avoided by mass selection and collisional activation of the purine base fragment ion as a precursor species, which results in extensive dissociation of the heterocyclic ring.[12-16] The resulting CID mass spectra permit clear differentiation of methylated purine isomers as well as other analytical applications,[2,17,18] as earlier demonstrated for methyladenine isomers.[19,20] Of particular relevance to the present study is the CID mass spectrum of protonated adenine,[21] which shows major dissociation reactions involving formation of NH_4^+ and loss of NH_3 and NH_2CN, which arise by unknown mechanisms, and are essentially absent in the EI mass spectrum of adenine.[23] Similar major

* To whom correspondence should be addressed at the Department of Medicinal Chemistry, Skaggs Hall, University of Utah, Salt Lake City, UT 84112.

(1) Schram, K. H. In *Mass Spectrometry*; Lawson, A. M., Ed.; Walter de Gruyter: New York, 1989; pp 507-570.
(2) Crain, P. F. *Mass Spectrom. Rev.* **1990**, *9*, 505-554.
(3) Crain, P. F.; Hashizume, T.; Nelson, C. C.; Pomerantz, S. C.; McCloskey, J. A. In *Biological Mass Spectrometry*; Burlingame, A. L., McCloskey, J. A., Eds.; Elsevier: New York, 1990; pp 509-526.
(4) McCloskey, J. A. *Acc. Chem. Res.* **1991**, *24*, 81-88.
(5) For examples of the mass spectra of purine derivatives and related heterocycles, see: (a) Goto, M. In *Kagaku no Ryoiki*; Nankodo: Tokyo, 1968; Special Issue No. 85, pp 141-180. (b) *Mass Spectrometry of Heterocyclic Compounds*; Porter, Q. M., Ed.; Wiley: New York, 1985; Chapter 17.
(6) For examples and citations to earlier work involving electron ionization studies of adenine, see refs 7 and 8.
(7) Barrio, M. C. G.; Scopes, D. I. C.; Holtwick, J. B.; Leonard, N. J. *Proc. Natl. Acad. Sci. U.S.A.* **1981**, *78*, 3986-3988.
(8) Sethi, S. K.; Gupta, S. P.; Jenkins, E. E.; Whitehead, C. W.; Townsend, L. B.; McCloskey, J. A. *J. Am. Chem. Soc.* **1982**, *104*, 3349-3353.
(9) Hayes, R. N.; Gross, M. L. *Methods Enzymol.* **1990**, *193*, 237-263.
(10) Busch, K. L.; Glish, G. L.; McLuckey, S. A. *Mass Spectrometry/Mass Spectrometry: Techniques and Applications of Tandem Mass Spectrometry*; VCH Publishers: New York, 1988.
(11) Harrison, A. G.; Cotter, R. J. *Methods Enzymol.* **1990**, *193*, 3-37.
(12) Farmer, P. B. *Biomed. Environ. Mass Spectrom.* **1988**, *17*, 143-145.
(13) Sakurai, T.; Matsuo, T.; Kusai, A.; Nojima, K. *Rapid Commun. Mass Spectrom.* **1989**, *3*, 212-216.
(14) Hettich, R. L. *Biomed. Environ. Mass Spectrom.* **1989**, *18*, 265-277.
(15) Hocart, C. H.; Schlunegger, J. P. *Rapid Commun. Mass Spectrom.* **1989**, *3*, 249-254.
(16) Cushnir, J. R.; Naylor, S.; Lamb, J. H.; Farmer, P. B.; Brown, N. A.; Mirkes, P. E. *Rapid Commun. Mass Spectrom.* **1990**, *4*, 410-414.
(17) For review, see: Nelson, C. C.; McCloskey, J. A. *Adv. Mass Spectrom.* **1989**, *11B*, 1296-1308.
(18) Bozorgzadeh, M. J.; Beynon, J. H.; Wiebers, J. L. *Adv. Mass Spectrom.* **1980**, *8A*, 971-982.
(19) Schoen, A. E.; Cooks, R. G.; Wiebers, J. L. *Science* **1979**, *203*, 1249-1251.
(20) Ashworth, D. J.; Baird, W. M.; Chang, C.-J.; Ciupek, J. D.; Busch, K. L.; Cooks, R. G. *Biomed. Mass Spectrom.* **1985**, *12*, 309-318.
(21) Alexander, A. J.; Kebarle, P.; Fuciarelli, A. F.; Raleigh, J. A. *Anal. Chem.* **1987**, *59*, 2484-2491.
(22) Data are shown in the supplementary material.
(23) Rice, J. M.; Dudek, G. O. *J. Am. Chem. Soc.* **1967**, *89*, 2719-2725.

0002-7863/92/1514-3661$03.00/0

differences are apparent in both the high- and low-energy CID mass spectra of protonated guanine[13,24] compared with the EI mass spectrum,[23] as well as in the mass spectra of various alkylated purines.[25,26]

The present study was undertaken to examine the dissociation of protonated adenine following collisional activation, using models selectively labeled with ^{13}C, ^{2}H, and ^{15}N at each of the five nitrogen atoms. A number of experimental approaches[27] for ion collisional activation in either the low-energy (eV) or high-energy (keV) ranges of ion kinetic energy can in principal be used for dissociation experiments. The present study was carried out using electron-volt-range collision energies, with collision gas pressures set to produce primarily multiple collisions, because these conditions are most commonly used for structural and analytical applications in triple quadrupole, hybrid (magnetic sector–quadrupole), and ion trap instruments. For comparison, selected measurements were also made under single-collision conditions, to assess the effects of deposition of less internal energy,[9] with consequently reduced tendency for rearrangement or isomerization reactions.[28]

Detailed knowledge of fragmentation mechanisms of reactions induced by collisional activation is useful in understanding the origins of decomposition pathways emanating from MH^+ ions, in particular those pathways which do not occur in the case of odd-electron ($M^{\bullet+}$) ions. Understanding these reactions is also important for determining the extent to which a wealth of EI data on the mechanisms of dissociation of heterocycles might be used to interpret experiments involving CID of protonated molecules. Such information additionally serves as a basis for the potential applications of tandem mass spectrometry in studies of purine metabolism involving stable isotopes, and in the characterization of substituted adenine derivatives, which occur widely in diverse natural sources, including nucleoside antibiotics,[29] plant growth hormones,[30] and both RNA and DNA.[31] Because methylation is the most important form of natural modification in nucleic acids, adenine models methylated at the 1, 2, 3, 7, and N^6 positions have also been included in the present study, in order to determine the effects of methylation on the basic dissociation reactions of protonated adenine.

Results and Discussion

Collision-Induced Dissociation of Protonated Adenine. Site of Protonation of Adenine. In solution, adenine adopts the amino tautomeric form, and is protonated preferentially at N-1.[32,33] In the gas phase, adenine is highly basic with a proton affinity of 222–227 kcal/mol.[34] Ab initio calculations predict that the gas-phase structure is also the amino form, and the preferred protonation site remains at N-1[35,36] (structure **1**). Although **1**

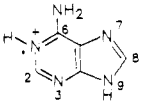

1

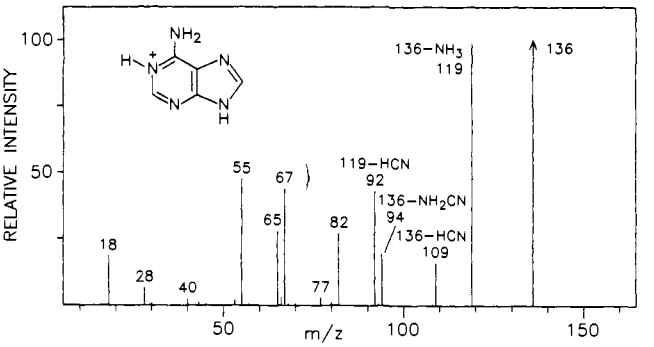

Figure 1. CID mass spectrum of protonated adenine (**1**), acquired under multiple-collision conditions.

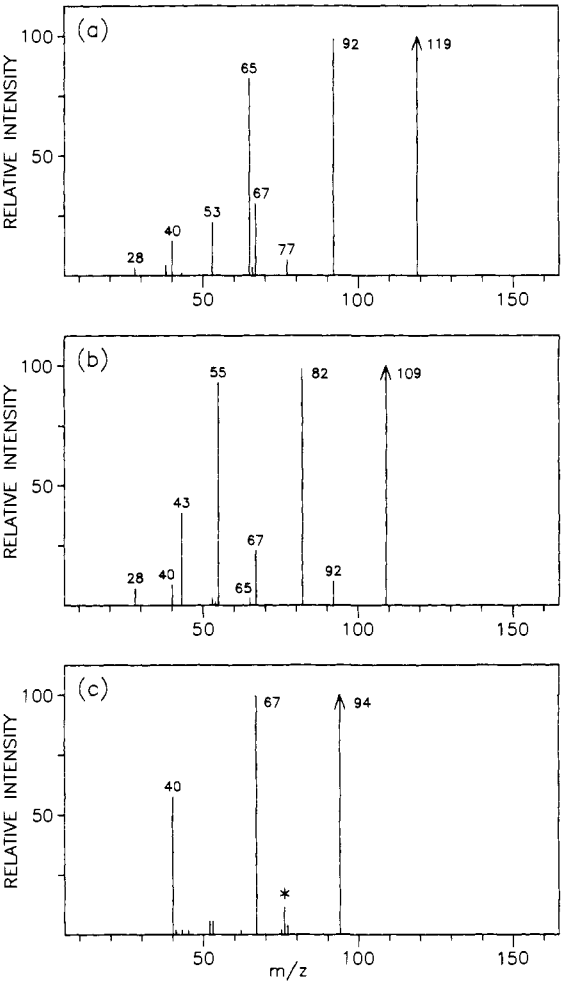

Figure 2. Mass spectra resulting from collision-induced dissociation of fragment ions representing the primary first-step dissociation products of protonated adenine. Precursor ions: (a) m/z 119, (b) m/z 109, and (c) m/z 94. Background ions are denoted by asterisks.

therefore reasonably represents the principal mass-selected species subjected to collisional activation, it is reasonable to assume that nitrogen basicities may change after opening of the pyrimidine ring, with opportunities for subsequent hydrogen migration and isomerization reactions concomitant with dissociation. Because of the occurrence of such hydrogen-transfer reactions, the CID mass spectra[22] of [2-^{2}H]- and [N^6,N^6,9-$^2H_3$]adenine were found to be less useful than ^{13}C or ^{15}N labeling of skeletal atoms in understaning the overall dissociation reactions.

(24) Ikonomou, M. G.; Naghipur, A.; Lown, J. W.; Kebarle, P. *Biomed. Environ. Mass Spectrom.* **1990**, *19*, 434–446.
(25) For example, see refs 19 and 20 and (a) Chang, C.-J.; Ashworth, D. J.; Isern-Flecha, I.; Jiang, X.-Y.; Cooks, R. G. *Chem.-Biol. Interact.* **1986**, *57*, 295–300. (b) Cushnir, J. R.; Naylor, S.; Lamb, J. H.; Farmer, P. B. *Rapid Commun. Mass Spectrom.* **1990**, *4*, 426–431.
(26) McCloskey, J. A. In *Basic Principles in Nucleic Acid Chemistry*; Ts'o, P. O. P., Ed.; Academic Press: New York, 1974; Vol. I, Chapter 3.
(27) For review, see ref 9.
(28) Kenttämaa, H. I. *Org. Mass Spectrom.* **1985**, *20*, 703–714.
(29) Isono, K. *J. Antibiot.* **1988**, *41*, 1711–1739.
(30) Letham, D. S.; Palni, L. M. S. *Annu. Rev. Plant Physiol.* **1983**, *34*, 163–197.
(31) *Chromatography and Modification of Nucleosides*; Gehrke, C. W.; Kuo, K. C. T., Eds.; Elsevier: New York, 1990.
(32) Ts'o, P. O. P. In *Basic Principles in Nucleic Acid Chemistry*; Ts'o, P. O. P., Ed.; Academic Press: New York, 1974; Vol. 1, p 453.
(33) Saenger, W. *Principles of Nucleic Acid Structure*; Springer-Verlag: Berlin. 1984; p 105.
(34) Wilson, M. S.; McCloskey, J. A. *J. Am. Chem. Soc.* **1975**, *97*, 3436–3444.
(35) Mezey, P. G.; Ladik, J. J.; Barry, M. *Theor. Chim. Acta* **1980**, *54*, 251–258.
(36) Del Bene, J. E. *J. Phys. Chem.* **1983**, *87*, 367–371.

Table I. Isotopic Compositions of Ions from Collision-Induced Dissociation of Selectively-Labeled Adenine

product ion	*m/z*	% isotope retained						
		N-1	N-3	N^6	N-7	N-9	C-2	H-2
$MH^+ - NH_3$	119	41	100	53	100	97	100	85
$MH^+ - NH_3 - HCN$	92[a]	44	52	29	86	83	50	31
$MH^+ - NH_3 - 2HCN$	65[a]	51	46	33	29	53	44	15
$MH^+ - NH_3 - C_2N_2$	67[a]	15	40	40	67	35	37	54
$MH^+ - NH_3 - NH_2CN$	77	44	76	23	29	25	77	33
$MH^+ - NH_2CN$	94	1	100	2	100	95	100	88
$MH^+ - HCN$	109	10	100	97	100	93	7	76
$MH^+ - 2HCN$	82	6	80	71	78	59	6	64
$MH^+ - 3HCN$	55	6	55	49	71	17	5	34
NH_4^+	18	89	2	8	0	0	0	96
H_2CN^+	28	23	11	8	25	32	26	50

[a] Alternate pathways also observed; see Scheme I.

Scheme I. Collision-Induced Dissociation Pathways of Protonated Adenine, Showing Primary Reaction Products (Open Arrows) and Secondary Products Determined by Mass Selection and Activation of Fragment Ions (Solid Arrows) or Implied by Elemental Composition Difference (Dashed Arrow)

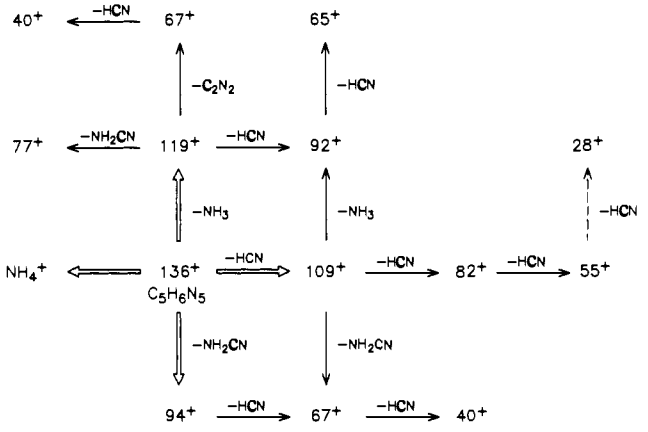

CID Mass Spectrum of Adenine. The mass spectrum resulting from collisional activation of protonated adenine, Figure 1, is qualitatively similar to that produced using atmospheric pressure chemical ionization with a triple quadrupole instrument.[21] The assignment of elemental compositions[22] to all ions in the spectrum is made possible by the mass shifts from the corresponding spectrum of [$^{15}N_5$]adenine,[22] supported by additional isotopic labeling data in the present study and by the high-resolution EI mass spectrum of adenine.[8] The main pathways of dissociation, shown in Scheme I, were determined by collisional activation of MH^+, and by direct analysis of the first-step dissociation product ions, shown in Figure 2, as well as from isotopic composition trends discussed below. Taken together with the principal ion assignments,[21] these data show four main dissociation pathways from the molecular ion: (i) loss of NH_3 (*m/z* 119) followed by two molecules of HCN (or HNC)[37] (*m/z* 92, 65); (ii) elimination of NH_2CN (*m/z* 94) and two molecules of HCN (*m/z* 67, 40); (iii) the sequential loss of three molecules of HCN (*m/z* 109, 82, 55); and (iv) formation of NH_4^+. All of these pathways except (iii) are trace processes in the EI mass spetrum of adenine[23,38] and in the CID mass spectrum of the odd-electron adenine molecular ion ($M^{\bullet+}$),[22] and therefore occur primarily as a consequence of protonation in the activated ion rather than from collisional activation alone. The sequential expulsion of HCN is a pathway common to many nitrogen heterocycles,[5] including adenine[23,38] and the parent compound purine.[39] Several lower mass ions, such as NH_4^+ (*m/z* 18) and H_2CN^+ (*m/z* 28), are difficult to distinguish from background in a conventional mass spectrum but are readily assigned in the tandem experiment in Figure 1.

(37) No distinction is presently made between HCN and HNC for structures of neutral species formed during dissociation.
(38) Shannon, J. S.; Letham, D. S. *N. Z. J. Sci.* **1966**, *9*, 833–842.
(39) Goto, T.; Tatematsu, A.; Matsuura, S. *J. Org. Chem.* **1965**, *30*, 1844–1846.

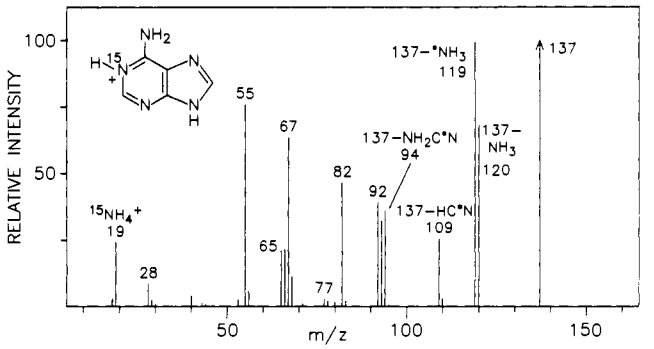

Figure 3. CID mass spectrum of protonated [1-^{15}N]adenine. Asterisk denotes ^{15}N isotope.

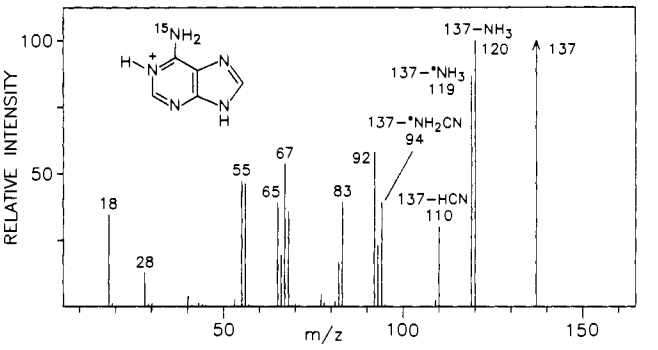

Figure 4. CID mass spectrum of protonated [6-*amino*-^{15}N]adenine. Asterisk denotes ^{15}N isotope.

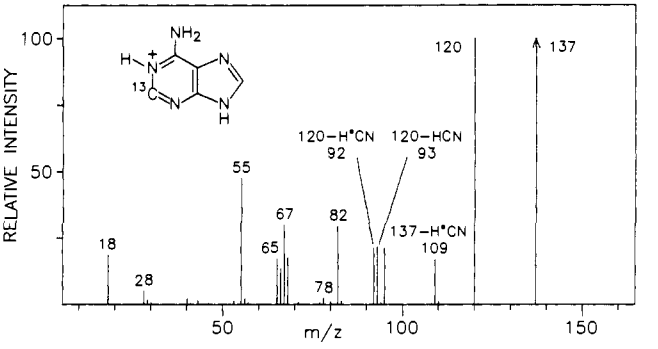

Figure 5. CID mass spectrum of protonated [2-^{13}C]adenine. Asterisk denotes ^{13}C isotope.

The site selectivity of the principal dissociation reactions was established primarily from the mass spectra of the five [^{15}N]-adenine isomers, resulting in the isotopic labeling distributions shown in Table I. The CID mass spectra of [1-^{15}N]adenine, [6-*amino*-^{15}N]adenine, and [2-^{13}C]adenine (Figures 3–5, respectively) are of particular importance, and reveal that initial steps in all four principal reaction paths involve dissociation of the pyrimidine moiety at N-1, as discussed below.[40]

Scheme II

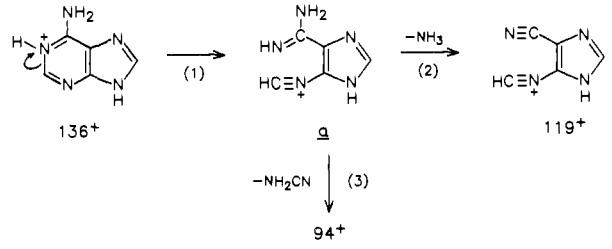

The labeling patterns in Table I show generally decreasing site specificity with regard to ^{15}N labels at progressively lower mass, indicating as might be expected, that some of the lower-mass ions which are produced by multistep processes are the result of converging reaction paths, for example, as shown in Scheme I for m/z 92 and 67. The complexity of reaction paths past the first dissociation steps is also reflected in several listings in Table I which imply small but significant consecutive increases (rather than decreases) in stable isotope content for the reaction sequence shown (e.g., the first three 1-^{15}N values of 41%, 44%, and 51%). Because the participation of each nitrogen atom is independently accounted for by ^{15}N labels, and unexpected intermediate reaction paths are not detected in Figure 2, we attribute apparent isotopic content increases as due to either minor isomerization reactions occurring in precursor ions or direct losses of larger neutral fragments of unknown structure from the molecular ion. In either case the isotopic contents of potential intermediate ions associated with such processes would be irrelevant. As a consequence of the increasing complexity and uncertainties associated with each step of multistep dissociation reactions, it is the initial reaction steps in each of the four principal pathways shown in Scheme I that are subject to reasonable analysis of the isotopic labeling data, and for which reaction mechanisms are presently proposed.

Loss of NH_3 and NH_2CN. As indicated in Table I, ammonia is expelled in approximately equal amounts from the ring nitrogen N-1 and the exocyclic nitrogen N^6, with little or no involvement of N-3, N-7, and N-9. Positional selectivity is also high for loss of cyanamide, shown by ^{15}N-labeling data to be essentially quantitatively derived from N-1 plus N^6, and by inference, C-6. The occurrence of these dissociation pathways, which are minor or nonexistent in both the EI[23] and CID mass spectra of the odd-electron molecular ion of adenine,[41] is interpreted in terms of ring-opening at the N-1–C-2 bond in the pyrimidine ring, shown as eq 1 of Scheme II.[42] This reaction is induced by protonation at N-1, which (independent of collisional activation) results in a major redistribution of electron density with predicted lengthening and thus weakening of the N-1–C-2 and C-2–C-6 bonds.[36] In the ring-opened intermediate a, N-1 and N^6 undergo partial loss of identity, leading to about 1:1 participation in expulsion of NH_3 to produce m/z 119 (eq 2). Alternatively, ion a may expel NH_2CN from the C-5 substituents with retention of one hydrogen to produce m/z 94 (eq 3).

Further loss of HCN from m/z 119 (Scheme I) leads to the m/z 92 ion which involves half of the C-2 and N-3 populations as revealed by isotopic labeling (and may include minor contributions from the alternate $109^+ \rightarrow 92^+$ route), but significant participation of other nitrogen and carbon atoms demonstrates the occurrence of additional competing mechanisms of dissociation, some of which require opening of the imidazole ring. It is then not surprising that the next loss of HCN ($92^+ \rightarrow 65^+$) is shown by labeling patterns to be yet less site-specific.

Scheme III

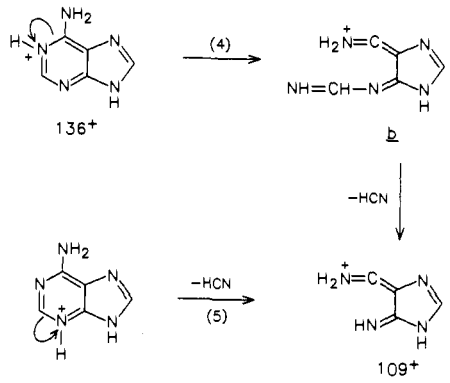

Sequential Elimination of HCN. Isotopic labeling data in Table I demonstrate that the first molecule of HCN eliminated occurs with approximately 90% specificity from N-1 plus C-2, and that second and third expulsions become increasingly less site-specific. We interpret the initial reaction primarily in terms of ring-opening of the N-1–C-6 bond as a result of protonation as shown in Scheme III (eq 4), followed by expulsion of HCN with retention of hydrogen to produce ion m/z 109. Surprisingly, deuterium labeling at C-2 demonstrates retention of approximately 24% of H-2 in this process, a value supported by the spectrum of [N^6,N^6,9-$^2H_3$]adenine[22] which shows loss of 77% DCN and 23% HCN. These data therefore clearly reveal migration of H-2 to the remainder of the heterocycle and its replacement by N-bound hydrogen, concomitant with expulsion of HCN.[43] Alternatively, it is possible that a minor population of molecular ions protonated at other sites (illustrated in eq 5 for convenience as N-3) may contribute to the m/z 109 ion population by direct expulsion of the N-1–C-2–H-2 group without necessity of hydrogen rearrangement.

Unlike the NH_3 and NH_2CN loss pathways, the expulsion of HCN is a major dissociation pathway common to both the odd-electron[23,38] ($M^{\cdot+}$) and even-electron[21] (MH^+) systems. It is therefore notable that the skeletal origin of the initially expelled HCN molecule in the present study is essentially the same as that demonstrated for $M^{\cdot+}$ ions:[7,8] 90% from N-1–C-2. This observation is extended qualitatively to the second loss of HCN ($109^+ \rightarrow 82^+$), which agrees with the odd-electron reaction data[8] ($108^+ \rightarrow 81^+$) in that N-3 and N-7 are the least involved nitrogen atoms in the elimination reaction.

The mass 67 ion ($C_3H_3N_2^+$) could in principle arise from the HCN pathway by loss of NH_2CN (Scheme I) in agreement with the earlier EI pathway established from spontaneous metastable ion dissociation,[8] or by elimination of HCN following initial loss of NH_2CN. On the basis of the CID of ion source-produced precursor ions (Figure 2b,c), both pathways $109^+ \rightarrow 67^+$ and $194^+ \rightarrow 67^+$ are observed. However, collisional activation of the m/z 119 ion revealed a third, unexpected pathway involving elimination of a 52-u neutral species. The composition C_2N_2 as shown in Scheme I was established from the 54-u mass difference for the analogous reaction $123^+ \rightarrow 69^+$ in the CID spectrum of m/z 123 of [$^{15}N_5$]adenine.[22] The significant involvement of N-3 and N-9 serves as further evidence for the increasing complexity of reaction paths past the initial decomposition step. Further dissociation of m/z 67 to form m/z 40 ($C_2H_2N^+$) was demonstrated[22] by mass selection and activation of the m/z 67 ion formed in the ion source. However, the two pathways for $67^+ \rightarrow 40^+$ shown in Scheme I, which involve ions of identical elemental composition, cannot be distinguished from the available data, and undoubtedly involve multiple ion structures and mechanisms. Additional minor pathways established from data shown in Figure 2 (omitted from

(40) Mass spectra of the remaining isomers, [3-^{15}N]-, [7-^{15}N]-, and [9-^{15}N]adenine, are of less relevance and are shown in the supplementary material.

(41) The CID mass spectrum derived from the odd-electron adenine molecular ion $M^{\cdot+}$ at 30-eV collision energy, shown in the supplementary material, shows % Σ (fragment ion) values of 56% for $M^{\cdot+} - NH_3$, 0.65% for $M^{\cdot+} - NH_2CN$, and 0.09% for NH_4^+.

(42) The structures shown in the schemes are largely diagrammatic in nature, and are not intended to rigorously depict actual ion structures, and do not portray isomerization or minor reactions which undoubtedly occur after initial ring-opening.

(43) The retention of carbon-bound hydrogen during loss of HCN from intermediate b (Scheme III) has an interesting parallel in the expulsion of HCN from protonated benzonitrile, as recently proposed: Wincel, H.; Fokkens, R. H.; Nibbering, N. M. M. *J. Am. Soc. Mass Spectrom.* **1990**, *1*, 225–232.

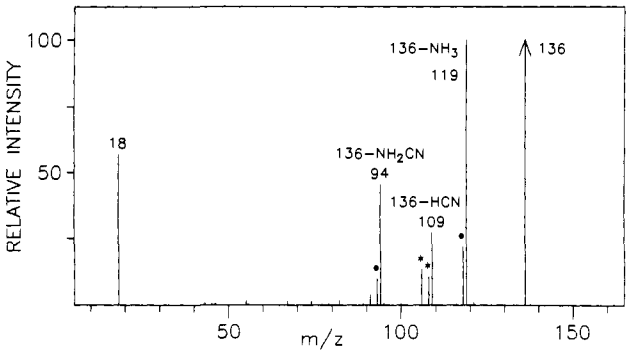

Figure 6. CID mass spectrum of protonated adenine (**1**), acquired under single-collision conditions. Background ions are denoted by asterisks.

Scheme I) are $109^+ \rightarrow 43^+$ ($CH_3N_2^+$) and $119^+ \rightarrow 53^+$ ($C_2HN_2^+$).

The prominent ammonium ion (m/z 18, Figure 1) is derived mainly from N-1 as shown in Table I, which is consistent with the role of N-1 as the initial site of protonation[35,36] and dissociation. Bearing four of the six hydrogens in protonated adenine, this ion is a remarkable product of the extensive hydrogen rearrangement, in which conformational flexibility of the ring-opened molecule permits transfer of three additional hydrogens to N-1. One of the hydrogen atoms is almost quantitatively (96%) derived from C-2.[22] The high hydrogen content of the ammonium ion, the absence of NH_4^+ as a product ion in Figure 2, and the selective incorporation of N-1 support the conclusion that it is a primary product of molecular ion dissociation, rather than an end product of multistep reactions. NH_4^+ is also formed at 4-eV collision energy,[22] as well as under single-collision conditions (Figure 6). These results indicate that the reaction is a surprisingly low energy process, and suggests that a significant population of ring-opened adenine ions may be formed in the ion source shortly after protonation.

Isotopic Compositions of Minor Product Ions. Isotopic compositions were measured for several lower-mass product ions, which clearly have multiple origins. Protonated HCN (m/z 28) exhibits relatively even contributions from ^{15}N (Table I), although somewhat less for N-3 and N^6, with an overall labeling pattern that is somewhat different from the H_2CN^+ species produced by electron ionization.[8] The minor m/z 77 ion corresponds in elemental composition to loss of NH_2CN from m/z 119, a conclusion supported by the spectrum in Figure 2a, but the distribution of ^{15}N labels as indicated in Table I clearly requires multiple mechanistic origins. Isotopic labeling data for five additional minor products (m/z 30, 40, 43, 45, 70) are listed in the supplementary material.

Dissociation of Protonated Adenine under Single-Collision Conditions. The amount of internal energy introduced by collision is a function of the number of collisions, so that single-collision conditions result in significantly lower total energy deposition for ions in the low-electronvolt translational energy range.[44] Although such conditions are often preferred in fundamental studies of collision processes, they are seldom used in structural or analytical work. At pressures used to define predominantly single-collision conditions, most ions undergo no collisions, leading to reduced sensitivity in terms of product ion current.

The effects of single-collision conditions on the dissociation of protonated adenine have been examined in order to determine the effect of relatively low internal energy on both the extent and mechanisms of dissociation, compared with results of multiple-collision experiments described above. The CID mass spectrum of protonated adenine was acquired at collision cell pressure corresponding to 15% beam reduction, resulting in predominantly single collisions. The product ion spectrum (Figure 6) indicates the occurrence of all four first-step dissociations shown in Scheme I, but with virtual absence of further decompositions. Comparison of the mechanisms of dissociation with those that pertain under multiple-collision conditions was made using the key labeled compounds [1-^{15}N]adenine and [6-*amino*-^{15}N]adenine. The results, shown in Table II, indicate that the pyrimidine ring, and N-1 in particular, remains as the principal site of dissociation and neutral molecule loss under single-collision conditions. Expulsion of NH_3 following ring-opening is much more selective than at higher internal energy (compare with Table I), with loss of N^6 much less favored than N-1, the site of protonation and opening of the pyrimidine ring. This result, in which the equivalence of N-1 and N^6 (see structure a, Scheme II) is reduced under conditions of lower internal energy, is in accord with earlier work by Kenttämaa who demonstrated that isomerization reactions in CID of bicyclic phosphate esters were substantially reduced under single-collision conditions, compared with those resulting from multiple collisions.[28] By contrast, the expulsion of HCN, while occurring predominantly from N-1 (Table II), is slightly less selective than under multiple-collision conditions (Table I). This difference is interpreted in terms of the higher internal energy requirement to form the precursor for HCN loss from N-1, which is thus less favored under single-collision conditions. The isotopic compositions shown in Table II for the ammonium ion and for the product of cyanamide expulsion are qualitatively the same as in Table I, showing these site-selective processes to reflect relatively less dependence on internal energy content, for collisions in the electronvolt range.

Table II. Isotopic Compositions of Ions Produced under Single-Collision Conditions from [1-^{15}N]- and [6-*amino*-^{15}N]Adenine

product ion	m/z	% ^{15}N retained	
		N-1[a]	N^6
$MH^+ - NH_3$	119	13	75
$MH^+ - HCN$	109	22	78
$MH^+ - NH_2CN$	94	9	3
NH_4^+	18	93	8

[a] Values shown for 1-^{15}N are subject to approximately ±5% ^{15}N error due to presence of minor matrix ions.

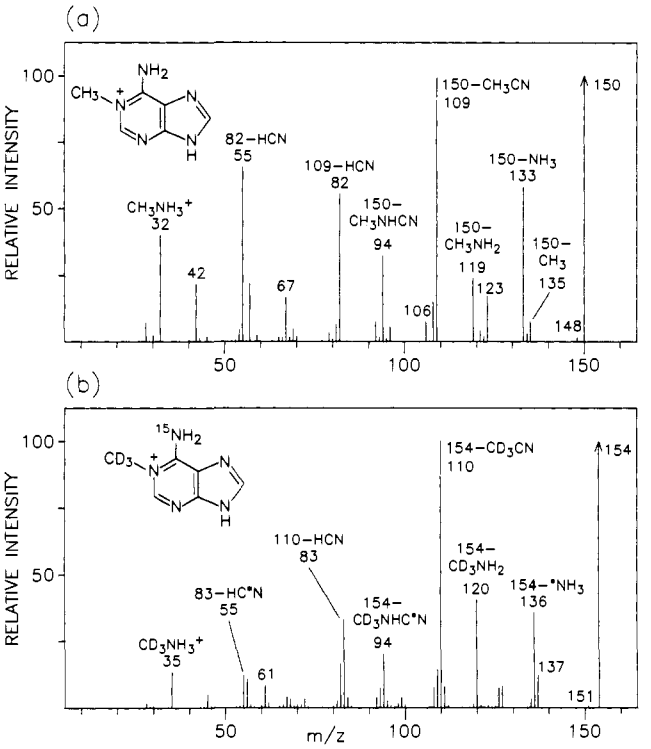

Figure 7. CID mass spectra of protonated (a) 1-methyladenine (**2**), (b) 1-([$^2H_3$]methyl)[6-*amino*-^{15}N]adenine (**5**). Asterisk denotes ^{15}N isotope. The peak at m/z 136 includes a minor contribution due to loss of CD_3 from m/z 154.

Collision-Induced Dissociation of Protonated Methyladenine Isomers. Mass spectra were acquired following collisional acti-

(44) Wysocki, V. H.; Kenttämaa, H. I.; Cooks, R. G. *Int. J. Mass Spectrom. Ion Processes* **1987**, *75*, 181-208.

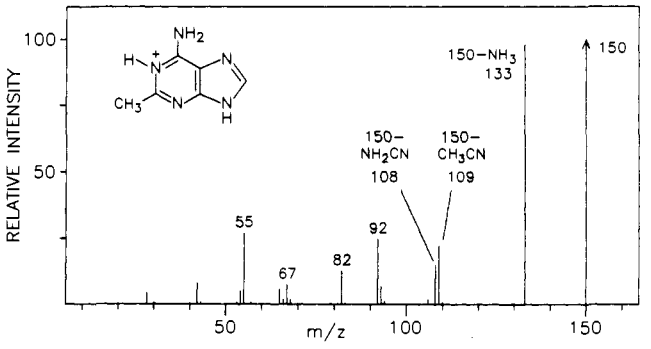

Figure 8. CID mass spectrum of protonated 2-methyladenine (**3**).

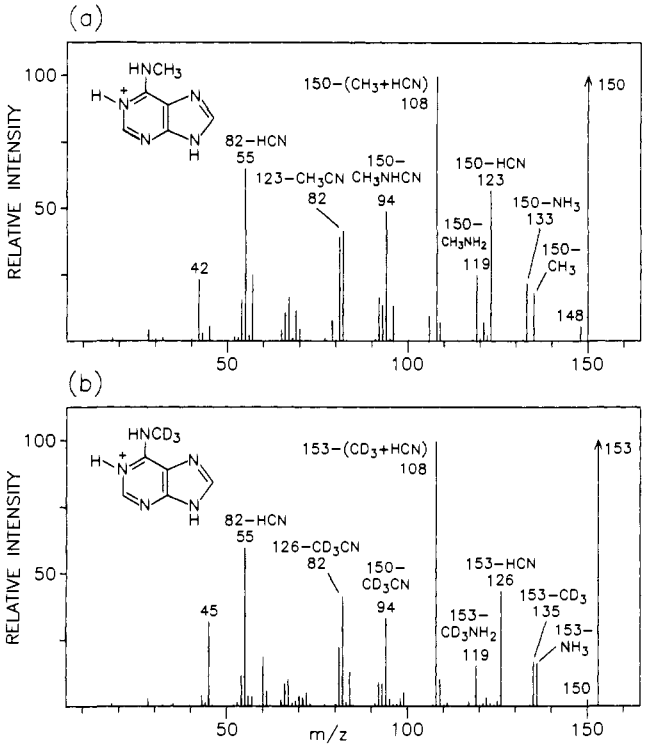

Figure 9. CID mass spectra of protonated (a) N^6-methyladenine (**4**) and (b) N^6-([$^2H_3$]methyl)adenine (**6**).

vation of protonated adenine methylated at positions N-1 (**2**, Figure 7a), C-2 (**3**, Figure 8), N-3,[22] N^6 (**4**, Figure 9a), and N-7.[22]

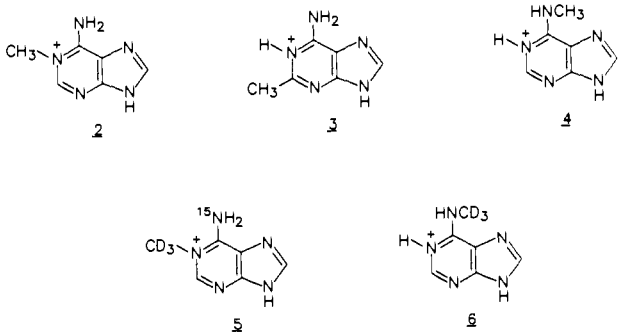

As discussed below, the principal reaction paths are best interpreted in terms of opening of the pyrimidine ring due to an initial charge at N-1, in direct analogy to adenine, and in agreement with N-1 as the preferred site of protonation (or charge site as shown for **2** (ref 32)). Therefore, the present study was focused on **2**–**4** (which also represent the principal sites of methylation of adenine in nucleic acids), and on the selectively-labeled precursor ions **5** and **6** (Figures 7b and 9b). The CID mass spectra in Figures 7a, 8, and 9a are qualitatively similar to the corresponding mass-analyzed ion kinetic energy (MIKE) spectra resulting from high-energy collisions.[19,45] To some extent, differences between mass spectra from the present study and the corresponding EI mass spectra[26] can, as in the case of adenine, be attributed to the role of protonation in generating different reaction channels. These differences include the following: (i) absence of HCN expulsion from $M^{\bullet+}$ from any methyladenine isomer, which is common when the precursor ion is MH^+; (ii) the elimination of methylenimine from the 6-methylamino moiety, which is a favorable and structurally diagnostic process in EI spectra[46] but is of minor importance in Figure 9a;[47] (iii) simple loss of $CH_3^\bullet$ from nitrogen (m/z 135 in Figures 7a and 9a) is not observed from $M^{\bullet+}$, which would result in placing a formal positive charge on nitrogen; and (iv) loss of $H^\bullet$ from the N^6- and 7-methyl isomer $M^{\bullet+}$ ions, evidently not a simple process,[26] is absent when the precursor ion is protonated.

Scheme IV

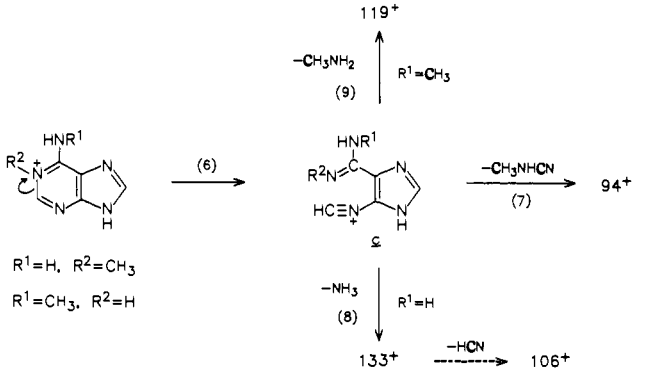

Table III. Influence of Site of Substitution on Loss of HCN from Protonated Methyladenines

position of methylation	relative abundance	
	$MH^+ - CH_3CN$	$MH^+ - HCN$
N-1	85	15
C-2	100	0
N-3	35	65
N^6	11	89
N-7	0	100

Dissociation Pathways Analogous to Adenine. Mass spectra of the 1-methyl (**2**) and N^6-methyl (**4**) isomers (Figures 7a and 9a) show product ions consistent with loss of NH_3 (m/z 133), CH_3NH_2 (m/z 119), and CH_3NHCN (m/z 94). The assignment for m/z 94 is supported by isotopic labeling (Figures 7b and 9b) which demonstrates loss of the methyl group, and in the case of **5**, of the 6-amino nitrogen as well. As shown in Scheme IV we interpret these results in terms of pyrimidine ring-opening (eq 6) followed by elimination of CH_3NHCN (eq 7), in direct analogy to eq 3. Alternatively, the opened intermediate c may expel either NH_3 (eq 8) or CH_3NH_2 (eq 9)[48] in correspondence to eq 2 of Scheme II. In Figure 7b the isotopic labeling pattern representing ammonia loss shows $^{15}NH_3$ elimination (m/z 136) to be favored over NH_3 (m/z 137), with the dominant reaction (loss of $^{15}NH_3$) not requiring rearrangement. This process bears some analogy to the expulsion of NH_3 from either N-1 or N^6 in Scheme II in which loss of N-1 is favored, but which is diminished in the case

(45) MIKES spectra published in ref 19 were used for the purpose of differentiation of the three methyladenine isomers and were not interpreted. Although resolution limitations inherent in the MIKES technique prevent detailed comparison with mass spectra from the present study, the principal differences appear to be the presence of m/z 120 as a major ion from **2** and **4** (absent in Figures 6a and 8a) and the presence of m/z 135 from **3** (absent in Figure 8).

(46) For leading references, see: von Minden, D. L.; Liehr, J. G.; Wilson, M. H.; McCloskey, J. A. *J. Org. Chem.* **1974**, *39*, 285–289.

(47) The assignment of m/z 121 as due to loss of $CH_2{=}NH$ is supported by the mass shift to m/z 123 in Figure 9b, in analogy to earlier results from EI experiments.[46]

(48) No distinction based on the present data can be made for the contribution from an alternate pathway for formation of m/z 119 by loss by $CH_2{=}NH$ from ion m/z 148.

of **2** because of the requirement for methyl rearrangement from N-1. The isotopic purity of the m/z 200 region in Figure 7b shows that methylamine expulsion occurs from intermediate c with negligible methyl migration to N^6.

In the mass spectra of methyladenine isomers, dissociation processes corresponding to elimination of the first molecule of HCN in Scheme III are represented by two potential pathways which result from methylation: loss of CH_3CN to produce m/z 109 and loss of HCN to produce m/z 123. The occurrence of these product ions in the mass spectra of the five isomers demonstrates a strong dependence on the site of methylation, which is summarized in Table III. We interpret these results in analogy to initial opening of the N-1–C-6 bond in eq 4 of Scheme III, as follows. In the case of **2**, the high site specificity for loss of the N-1 plus C-2 atoms is reflected (Table III) in elimination of CH_3CN as the major process. Although alternative loss of HCN could in principal come from other parts of the molecule, we believe it likely to still involve N-1 plus C-2, concomitant with methyl migration from N-1 (equivalent to migration of H from N-1 prior to loss of HCN from adenine in eq 4 as earlier discussed). By contrast, when C-2 is methylated, the loss of HCN would require rearrangement of CH_3 from carbon, a much less likely process, so that initial HCN loss is uniquely absent in the spectrum of the 2-methyl isomer as shown in Figure 8. In the spectra of the N^6- and 3-methyl isomers, elimination of HCN predominates as expected, while protonated 7-methyladenine loses HCN exclusively, further confirming the pyrimidine ring as the principal reaction site of initial dissociation. Following the first loss of either CH_3CN or HCN, additional multistep eliminations of HCN occur, shown by isotopic labeling patterns (Figures 7b and 9b), to involve increasingly less site selectivity, as expected from adenine results.

Methylation at N-1 of the purine nucleus results in a notable shift of the NH_4^+ from adenine (Figure 1) to m/z 32 only in the mass spectrum of **2** (Figure 7a), in agreement with the finding that N-1 is the principal contributor to NH_4^+ as indicated previously.

Other Product Ions Associated with Methylation. All of the *N*-methyladenine isomers are observed to lose a $CH_3^\bullet$ radical, although in the case of 7-methyladenine it is a minor process. (The overall extent of fragmentation of 7-methyladenine was notably less than for other isomers under the same conditions.) The product ion resulting from N-demethylation is then formally equivalent to the adenine odd-electron molecular ion, $M^{\bullet+}$, from EI. Loss of $CH_3^\bullet$ from C-2 is not observed (Figure 8) as would be reasonably expected, although it does occur following kilovolt-range collisional activation.[19] Interestingly, loss of $CH_3^\bullet$ to yield the $(M - CH_3)^{\bullet-}$ radical ion is a major process in the negative ion CID mass spectra of deprotonated methyladenine $(M - H)^-$ ions.[15] In Figure 9a, the principal product ion (m/z 108) results from methyl radical loss, in combination with elimination of HCN, and appears to be a minor ion in the mass spectrum of the 1-methyl isomer (Figure 7a). Additional information on the mechanism of formation of m/z 108 would require further isotopic labeling to establish the origin of HCN.

The elimination of a molecule of H_2 in the dissociation of 1- and N^6-methyladenines (Figures 7a and 9a) is an unusual minor reaction, but which is consistent with formation of intermediate c in Scheme IV. The results of deuterium labeling in the methyl groups of **5** and **6** reveal elimination of HD (Figures 7b and 9b). This reaction can occur between methyl hydrogen and the two N-bound hydrogens in the N-1–C-6–N^6 portion of the intact cyclic molecular ion, or more readily from the N–C-6–N substituents in intermediate c by any of several possible mechanisms.

Experimental Section

General Remarks and Materials. Isotopic purity of all labeled compounds was approximately 99 atom % or greater. The following were obtained from commercial sources: adenine, 1-, 2-, and 3-methyladenines, 1-methyladenosine, and N^6-methyladenosine (Sigma, St. Louis, MO); [2-^{13}C]adenine, [2-^{2}H]adenosine, and *O*-perdeuterioglycerol (MSD Isotopes, St. Louis, MO); N^6-methyladenine (Vega Biochemicals, Tucson, AZ); and 7-methyladenine (Cyclo Chemical Corp., Los Angeles, CA). Syntheses of the following labeled models were carried out by S. P. Gupta and previously described in ref 8: [1-^{15}N]adenine, [3-^{15}N]adenine, [6-*amino*-^{15}N]adenine, [7-^{15}N]adenine, and [9-^{15}N]adenine. 1-([$^2H_3$]-Methyl)[6-*amino*-^{15}N]adenosine and N^6-([$^2H_3$]methyl)adenosine were prepared by M. H. Wilson for earlier studies, as described.[49] [1,3,N^6,7,9-$^{15}N_5$]Adenine ([per-^{15}N]adenine) was a gift from A. L. Nussbaum, Hoffmann-LaRoche Inc., Nutley, NJ. [N^6,N^6,9-$^2H_3$]-Adenine was prepared by mixing adenine with *O*-perdeuterioglycerol on a mass spectrometer sample probe tip for analysis by FAB mass spectrometry, by procedures earlier described.[50,51]

Mass Spectrometry. CID mass spectra were acquired using a VG-70SEQ instrument, consisting of a double-focusing magnetic sector mass analyzer (MS-1), rf-only quadrupole gas collision cell, and quadrupole mass analyzer (MS-2), controlled by a VG-11/250J data system. All samples were dissolved in glycerol and ionized by fast atom bombardment (FAB) by Xe, using a saddle-field-type FAB gun (model FAB 11N, Ion Tech Ltd., Middlesex, U.K.) operated at 7.2–7.6 kV and 1.1-mA discharge current. Precursor ions were mass-selected using MS-1 operated at resolution 1000. All CID spectra recorded by MS-2 were acquired at unit mass or greater resolution, and mass spectra were signal-averaged over five scans.

CID mass spectra were produced using 30-eV translational energy (E_{LAB}) of the incident precursor ion at a collision gas pressure corresponding to transmission of approximately 20% of the precursor ion beam, resulting in predominantly multicollision conditions. For measurements made under single-collision conditions (Figure 6 and Table II), pressures resulting in 85–90% transmission were used, at 25–30-eV energy. Argon was used as the collision gas for all adenine measurements except those using [2-^{2}H]adenosine and [N^6,N^6,9-$^2H_3$]adenine, and krypton was used for all other experiments and for single-collision measurements. The collision cell pressure for each series was set to the same value using an Edwards Ion-7 ionization gauge by monitoring pressure in close proximity to the collision cell.

The isotopically labeled ions **5** and **6** and protonated [2-^{2}H]adenine were prepared from the corresponding 9-β-D-ribofuranosides as fragment ions produced in MS-1 following FAB ionization. The assumption that the nucleoside-derived fragment ion **5** is structurally identical to the MH^+ ion from the corresponding base was validated[52,53] by showing that the CID mass spectrum from **2** derived from the protonated base is indistinguishable from that produced from **2** generated from 1-methyladenosine.[22] These results are in accord with earlier measurements carried out using odd-electron base ions formed by electron ionization,[8,54] which showed analogous equivalence between base fragments and molecular ions of the free bases.

Isotopic Composition Calculations. Isotopic compositions listed in Tables I and II were calculated as percentages of total ion current for each ion species. Therefore, % isotope retained = $100a/(a + b)$, where a = abundance of labeled ion and b = abundance of unlabeled ion 1 u lower. The accuracy of isotopic composition values given in Tables I and II depends on ion abundances and signal-to-background ratios, but are generally within ±3% (i.e., 41 ± 3% for the first entry in Table I).

Acknowledgment. This work was supported by Grant GM 21584 from the National Institutes of Health. We are grateful to Drs. S. P. Gupta and M. H. Wilson who prepared some of the isotopically labeled compounds in conjunction with earlier studies, and to S. C. Pomerantz for structural drawings.

Registry No. Adenine, 73-24-5; 1-methyladenine, 5142-22-3; 2-methyladenine, 1445-08-5; 3-methyladenine, 5142-23-4; 1-methyladenosine, 15763-06-1; N^6-methyladenosine, 18769-73-8; [2-^{13}C]adenine, 97908-72-0; [2-^{2}H]adenosine, 109923-50-4; N^6-methyladenine, 443-72-1; 7-methyladenine, 935-69-3; [1-^{15}N]adenine, 79364-53-7; [3-^{15}N]adenine, 79364-54-8; [6-*amino*-^{15}N]adenine, 19713-11-2; [7-^{15}N]adenine, 79364-55-9; [9-^{15}N]adenine, 56777-22-1; 1-([$^2H_3$]methyl)[6-*amino*-^{15}N]adenosine, 139896-42-7; N^6-([$^2H_3$]methyl adenosine, 139896-43-8; [1,3,N^6,7,9-$^{15}N_5$]adenine, 77910-29-3; [N^6,N^6,9-$^2H_3$]adenine, 51581-02-3.

Supplementary Material Available: CID mass spectra of protonated [per-^{15}N]adenine, [3-^{15}N]adenine, [7-^{15}N]adenine, [9-^{15}N]adenine, [N^6,N^6,9-$^2H_3$]adenine, adenine at 4-eV collision

(49) Wilson, M. H.; McCloskey, J. A. *J. Org. Chem.* **1973**, *38*, 2247–2249.
(50) Sethi, S. K.; Smith, D. L.; McCloskey, J. A. *Biochem. Biophys. Res. Commun.* **1983**, *112*, 126–131.
(51) Verma, S.; Pomerantz, S. C.; Sethi, S. K.; McCloskey, J. A. *Anal. Chem.* **1986**, *58*, 2898–2902.
(52) Levsen, K.; Schwartz, H. *Angew. Chem., Int. Ed. Engl.* **1976**, *15*, 509–568.
(53) Holmes, J. L. *Org. Mass Spectrom.* **1985**, *20*, 169–183.
(54) Puzo, G.; Wiebers, J. L. *Nucleic Acids Res.* **1981**, *9*, 4655–5667.

energy, 3-methyladenine, and 7-methyladenine, base fragment ions from [2-^{2}H]adenosine and 1-methyladenosine, ion source produced adenine fragment ions m/z 67 and 82 and [per-^{15}N]-adenine fragment ions m/z 113 and 123, protonated [1-^{15}N]-adenine and [6-*amino*-^{15}N]adenine under single-collision conditions, and the odd-electron molecular ion ($M^{\bullet+}$) of adenine and tables of elemental compositions of ions produced by CID of protonated adenine and isotopic compositions of minor ions from CID of isotopically labeled adenines (8 pages). Ordering information is given on current masthead page.

Molecular Dynamics Studies of Calixspherand Complexes with Alkali Metal Cations: Calculation of the Absolute and Relative Free Energies of Binding of Cations to a Calixspherand

Shuichi Miyamoto and Peter A. Kollman*

Contribution from the Department of Pharmaceutical Chemistry, University of California, San Francisco, California 94143. *Received August 22, 1991*

Abstract: We present molecular dynamics studies of the complexation of a macrobicyclic calixspherand host with guest metal cations (Na^+, K^+, and Rb^+). By using a thermodynamic free energy perturbation method, the relative free energies of calixspherand complexation with alkali metal cations were determined. We tested two sets of van der Waals parameters, two methods of describing 1-4 nonbonded interactions and two extreme models of solvation for the calixspherand-alkali ion complex. Independent of model, the calculations correctly reproduced the tighter binding to the calixspherand of K^+ compared to the smaller Na^+ and the larger Rb^+. Encouragingly, the "best model" (most highly refined ion parameters, most complete description of solvation) gave the best quantitative reproduction of the experimental free energies. We have also carried out the first example of the calculation of the absolute binding free energy of a macrobicyclic molecule-ion complex. The absolute binding free energy of the calixspherand·Rb^+ complex was calculated to be -11 to -13 kcal/mol, in good agreement with experiment (-12 to -13 kcal/mol). In addition to reproducing the observed K^+ selectivity and shedding light on the experimental free energy data, ion-oxygen radial distribution functions derived from molecular dynamics simulations on the ions, Na^+, K^+, and Rb^+, both in water and in the calixspherand, allowed clear insight into the K^+ preference for this calixspherand. Only for K^+ does the first peak of the ion-oxygen radial distribution function in the host coincide with that in water; for Na^+, the first peak is at a larger distance in the host than in water; for Rb^+, the first peak is at a smaller distance in the host than in water. Both the free energy and structural results further emphasize the delicate balance between ion-water and ion-host interactions that lead to ion selectivity.

Introduction

The ability of synthetic receptor molecules such as macrocyclic polyethers to complex cations or anions has received much attention during the last two decades.[1] The complexation properties of these hosts with a variety of guest molecules have been reported. Cram has reviewed two principles that govern the complexation process: complementarity and preorganization.[2] Complementarity involves the steric and electrostatic fit of host and guest; for complexation of macrocyclic polyethers with metal cations, complementarity is reflected by a cavity-shape cation-size relationship. Preorganization is defined as the absence of structural reorganization and desolvation of the host upon complexation; the more highly hosts organized for binding and for low solvation prior to their complexation, the more stable will be their complexes. Application of this preorganization principle has led to the synthesis of the spherands.[3]

Recently Reinhoudt et al. have presented the synthesis, thermodynamics, and kinetics of binding and X-ray crystal structures of a series of calixcrowns and calixspherands and have demonstrated that calixspherand **1** (Chart I) forms the most stable complex with alkali metal cations of this class of structures.[4] X-ray and NMR studies on **1** indicate that the *m*-teranisyl moiety has an alternating arrangement of the three methoxy oxygen atoms, and the 1,3-dimethoxy-*p*-*tert*-butylcalix[4]arene moiety has a flattened partial cone conformation[5] both in free state and after complexation with alkali cations. For this reason, compound **1** can be considered a highly preorganized host molecule. The free energies of complexation of **1** with alkali picrates (in $CDCl_3$) derived from the NMR studies[4b] at 298 K are -16.8 (**1**·Na^+), -18.1 (**1**·K^+), and -13.0 (**1**·Rb^+) kcal/mol, respectively, while free energies of -13.6, -14.0, and -12.0 kcal/mol, respectively, were determined by the picrate extraction experiments.[4a] In both cases the selectivity of **1** for K^+ was observed.

A theoretical technique, the thermodynamic perturbation method,[6] has been applied to a variety of host-guest systems and

(1) For some recent reviews with leading references, see: (a) Cram, D. J. *Science* **1988**, *240*, 760-767. (b) Diederich, F. *Angew. Chem., Int. Ed. Engl.* **1988**, *27*, 362-386. (c) Lehn, J. M. *Angew. Chem., Int. Ed. Engl.* **1988**, *27*, 89-112. (d) Rebek, J., Jr. *Science* **1987**, *235*, 1478-1484. (e) Colquhoun, H. M.; Stoddart, J. F.; Williams, D. J. *Angew. Chem., Int. Ed. Engl.* **1986**, *25*, 487-507.

(2) (a) Cram, D. J.; Trueblood, K. N. *Top. Curr. Chem.* **1981**, *98*, 43. (b) Cram, D. J. *Angew. Chem., Int. Ed. Engl.* **1986**, *25*, 1039-1157.

(3) (a) Trueblood, K. N.; Knobler, C. B.; Maverick, E.; Helgeson, R. C.; Brown, S. B.; Cram, D. J. *J. Am. Chem. Soc.* **1981**, *103*, 5594-5596. (b) Cram, D. J.; Lein, G. M.; Kaneda, T.; Helgeson, R. C.; Knobler, C. B.; Maverick, E.; Trueblood, K. N. *J. Am. Chem. Soc.* **1981**, *103*, 6228-6232. (c) Lein, G. M.; Cram, D. J. *J. Chem. Soc., Chem. Commun.* **1982**, 301.

(4) (a) Reinhoudt, D. N.; Dijkstra, P. J.; in't Veld, P. J. A.; Bugge, K.-E.; Harkema, S.; Ungaro, R.; Ghidini, E. *J. Am. Chem. Soc.* **1987**, *109*, 4761-4762. (b) Dijkstra, P. J.; Brunink, J. A. J.; Bugge, K.-E.; Reinhoudt, D. N.; Harkema, S.; Ungaro, R.; Ugozzoli, F.; Ghidini, E. *J. Am. Chem. Soc.* **1989**, *111*, 7567-7575. (c) Ghidini, E.; Ugozzoli, F.; Ungaro, R.; Harkema, S.; El-Fadl, A. A.; Reinhoudt, D. N. *J. Am. Chem. Soc.* **1990**, *112*, 6979-6985.

(5) Gutsche, C. D. *Prog. Macrocycl. Chem.* **1987**, *3*, 93-165.

(6) (a) Tembe, B. L.; McCammon, J. A. *Comput. Chem.* **1984**, *8*, 281. (b) Bash, P. A.; Singh, U. C.; Langridge, R.; Kollman, P. A. *Science* **1987**, *236*, 564-568. (c) McCammon, J. A. *Science* **1987**, *238*, 486-491. (d) Straatsma, T. P.; Berendsen, H. J. C. *J. Chem. Phys.* **1988**, *89*, 5876-5886. (e) Jorgensen, W. L.; Briggs, J. M. *J. Am. Chem. Soc.* **1989**, *111*, 4190-4197. (f) Aqvist, J.; Warshel, A. *Biophys. J.* **1989**, *56*, 171-182. (g) Owenson, B.; Macelroy, R. D.; Pohorille, A. *J. Mol. Struct.* **1988**, *179*, 467-484.

0002-7863/92/1514-3668$03.00/0